

JOURNAL OF SCIENCE



SAKARYA UNIVERSITY

Sakarya University Journal of Science

ISSN 1301-4048 | e-ISSN 2147-835X | Period Bimonthly | Founded: 1997 | Publisher Sakarya University |
<http://www.saujs.sakarya.edu.tr/en/>

Title: Investigation of the Frequency and Voltage Dependent Dielectric Properties of Au/n-SiC Metal Semiconductor (MS) and Au/Al₂O₃/n-SiC Metal-Insulator-Semiconductor (MIS) Structures

Authors: Gülçin ERSÖZ DEMİR, İbrahim YÜCEDAĞ

Received: 2020-05-28 14:54:52

Accepted: 2020-08-08 00:30:38

Article Type: Research Article

Volume: 24

Issue: 5

Month: October

Year: 2020

Pages: 1040-1052

How to cite

Gülçin ERSÖZ DEMİR, İbrahim YÜCEDAĞ; (2020), Investigation of the Frequency and Voltage Dependent Dielectric Properties of Au/n-SiC Metal Semiconductor (MS) and Au/Al₂O₃/n-SiC Metal-Insulator-Semiconductor (MIS) Structures. Sakarya University Journal of Science, 24(5), 1040-1052, DOI:

<https://doi.org/10.16984/saufenbilder.744111>

Access link

<http://www.saujs.sakarya.edu.tr/en/pub/issue/56422/744111>

New submission to SAUJS

<http://dergipark.org.tr/en/journal/1115/submission/step/manuscript/new>



Investigation of the Frequency and Voltage Dependent Dielectric Properties of Au/n-SiC Metal Semiconductor (MS) and Au/Al₂O₃/n-SiC Metal-Insulator-Semiconductor (MIS) Structures

Gülçin ERSÖZ DEMİR^{*1}, İbrahim YÜCEDAĞ²

Abstract

In this study, we investigated the fabrication of Au/n-SiC (MS) and Au/Al₂O₃/n-SiC (MIS) type structures with atomic layer deposition (ALD) technique and their dielectric properties. The dielectric characteristics of structures were analyzed at frequency range of 1 kHz-500 kHz and by applying a (-3V)-(9V) bias voltage at 300 K. The significant dielectric parameters such as dielectric constant (ϵ') and dielectric loss (ϵ''), real and imaginary parts of electrical modulus (M' and M''), loss tangent ($\tan\delta$) were calculated by depending on frequency and voltage from capacitance-voltage ($C-V$) and conductance-voltage ($G/\omega-V$) data. Thereby, the effect of frequency on MS and MIS was searched in detail. The effect of the interface states occurred in the low frequency region can be attributed to the variation of the characteristic behavior of these parameters. It is clear that the dielectric parameters highly depend on the frequency and voltage at depletion and accumulation regions. Moreover, the peak position of M'' shifts to the left side of the graphic due to the effect of the insulating layer. It can be deduced from the obtained results that the interfacial polarization is easier at low frequencies. Also the interfacial polarization can contribute more to the variation of the dielectric properties.

Keywords: Au/Al₂O₃/n-SiC (MIS) type structures, AC electrical conductivity, Dielectric Properties, Impedance measurements.

1. INTRODUCTION

Metal-semiconductor (MS) structures which are used to determine the characteristic behavior of the semiconductor materials are significant investigation topics [1-4]. MS structures can be transformed into metal-insulator-semiconductor (MIS) structures through the insulator layer coated between metal and semiconductor. Interface

diffusion and reaction formed between the metal and semiconductor interface can be dramatically reduced because of the presence of an insulator layer. The structural properties of the insulator layer at the M/S interface, series resistance (R_s) and particular distribution of interface states between metal and semiconductor affect the electrical characteristics of the devices [5-7]. Degenerate bond structures in the semiconductor surface are

* Corresponding Author: glcnersoz@gmail.com

¹Department of Management Information Systems, Faculty of Management, Selçuk University, Konya 42700, Turkey. ORCID: <http://orcid.org/0000-0002-4813-4003>

²Department of Computer Engineering, Faculty of Technology, Düzce University, Düzce 81620, Turkey. E-Mail: yucedagi@gmail.com, ORCID: <http://orcid.org/0000-0003-2975-7392>

destroyed by the interfacial dielectric film. This dielectric film, which is between metal and semiconductor, decreases surface charge traps that are generally located at the Fermi level [8]. The alteration of barrier height by means of the presence of insulator layer on the M/S interface was ascribed to the interface dipole [9]. The performance, reliability and stability of the device are influenced predominantly because of the interfacial layer [10].

Among the different insulating materials, Aluminum oxide (Al_2O_3) nanomaterial has been regarded as one of the most promising materials due to its fabricate potential that has low-cost, stable and flexible electronic devices [11, 12]. Al_2O_3 has some interesting properties such as dielectric permeability (~ 9), wide band gap (9 eV) [13], and its formation of uniform interface with semiconductors. These provide the reduction of leakage of currents in devices, kinetics and thermodynamic stabilities of the semiconductor at high-temperatures. They also give rise to low interface defects as well as amorphous materials [14].

Techniques such as Sputtering, Spray pyrolysis, RF magnetron, electron beam evaporation, atomic layer deposition (ALD) were used to form Al_2O_3 thin films. The ALD technique is one of the most preferred methods for creating an interface layer with a high dielectric property on the substrate, since it has unique deposition characteristics such as precise thickness control, low impurity ratio, low processing temperature and excellent thickness uniformity on substrate areas [15-18]. Al_2O_3 thin film created by using the ALD showed excellent electrical properties. [18] The thin layers of Aluminum oxide obtained by the ALD technique have caught attention recently because of their excellent potential for highly effective and homogeneous surface passivation of semiconductor substrates [19-21]. Today, these kinds of devices generated by means of the silicon (Si) have been made convenient to daily usage as a result of long term studies. In spite of the great progress in material processing technology, device performance is confined due to the inadequacy of natural features in Si. To overcome this problem, there has been increasing necessity for studies into alternative materials to silicon (Si) to use in the power electronics. GaN, GaAs, and SiC are

materials that have emerged as alternatives to Si [22]. Among these materials, silicon carbide (SiC) semiconductor is mostly preferred because of its important properties in power electronic applications especially at the work with high voltage/temperature. Si and GaAs, based on appliances in power switching devices, have 8-10 times weaker performance than SiC based devices. This entails SiC to become a perfect candidate for these applications [23]. In general, MIS structure obtained from SiC is attractive due to low initial voltage (compared to SiC p-n diodes) and irreversibility.

According to literature, Al_2O_3 was used as interfacial layer on semiconductor substrates such as p-Si [24], n-Si [25], InP [26], n-GaAs [27], and SiC [28-30]. In this study, both Au/n-SiC metal/semiconductor (MS) and Au/ Al_2O_3 /n-SiC metal/insulator/semiconductor (MIS) type structures were produced by forming Al_2O_3 on n-SiC using the atomic layer deposition (ALD) technique. Therefore, we aimed to investigate dielectric and electrical behaviors of the Au/ Al_2O_3 /n-SiC type structures. Thereby, basic parameters such as the dielectric properties, electric modulus and conductivity of structures with and without Al_2O_3 interfacial layer were deeply investigated. For both structures, the permittivity (ϵ' and ϵ''), loss tangent ($\tan\delta$), electrical modulus (M' and M''), and ac electrical conductivity (σ_{ac}) parameters which depend on the frequency and voltage were researched on the frequency and voltage range of 1 kHz- 500 kHz and (-3V) - (9V), respectively, by measuring capacitance-voltage ($C-V$) and conductance-voltage ($G/\omega-V$) measurements at 300 K. Experimental results indicate that all these parameters are strong functions of frequency, voltage and Al_2O_3 interfacial layer.

2. MATERIALS AND METHODS

In this experimental work, n-Type, 8° off (0001) oriented, 4H-SiC wafers were used to produce the MS and the MIS type structures. Before the production of MS and MIS structures, wafers were sonicated for five minutes in acetone and five minutes in isopropanol and then rinsed in deionize (DI) water with resistivity of 18 $\text{M}\Omega\cdot\text{cm}$ for a prolonged time and wafers were dried under N_2 flow. After surface cleaning of n-4H-SiC high

purity Au (99.999%) was evaporated on the whole back of wafer by thermal evaporation method with 2000 Å at 1×10^{-6} Torr. In order to get low resistivity ohmic back contact, Au coated wafers were annealed at 500°C in the nitrogen ambient. Then, they were prepared with atomic layer deposition (ALD) system for Al₂O₃ coating on MS type structure. Under UV radiation, deposition process was carried out and it was heated at 370°C using trimethylaluminum and water. The deposited Al₂O₃ thickness was 70 Å. Finally, high purity Au was deposited on the Al₂O₃ at 1×10^{-6} Torr in the same thermal evaporation system. In order to perform electrical measurements of these MS and MIS type structures, the fabricated samples were mounted on a copper holder with the help of silver dag. The electrical contacts were made to the upper electrodes by use of tiny silver coated wires with silver paste. The forward and reverse bias $C-V$ and $G/\omega-V$ measurements were obtained by using an HP4192A LF impedance meter in the frequency range of 1 kHz-500 kHz. All measurements were realized with the help of a microcomputer through an IEEE-488 AC/DC converter card.

3. RESULT AND DISCUSSION

The forward (9V) and reverse (-3V) bias voltage $C-V$ measurements of Au/n-SiC (MS) and Au/Al₂O₃/n-SiC (MIS) structures were obtained by using an HP4192A LF impedance meter in the frequency range of 1 kHz-500 kHz at 300 K. The obtained results were presented in Fig.1 (a) and (b), respectively. When the Figs. 1 (a) and (b) are carefully examined, it can be seen that the obtained C values are strongly dependent on frequency in depletion and accumulation regions. The C values of the MS and MIS structures decrease with increasing frequency. These behaviors were ascribed to traps in the interface between metal and semiconductor.

Although the capacitance of the MS structure reaches a maximum value, it does not have a peak in depletion region. Fig. 1 (b) shows that a dielectric interface layer between the metal and the semiconductor corrects the capacitance behavior of the MS structure [31].

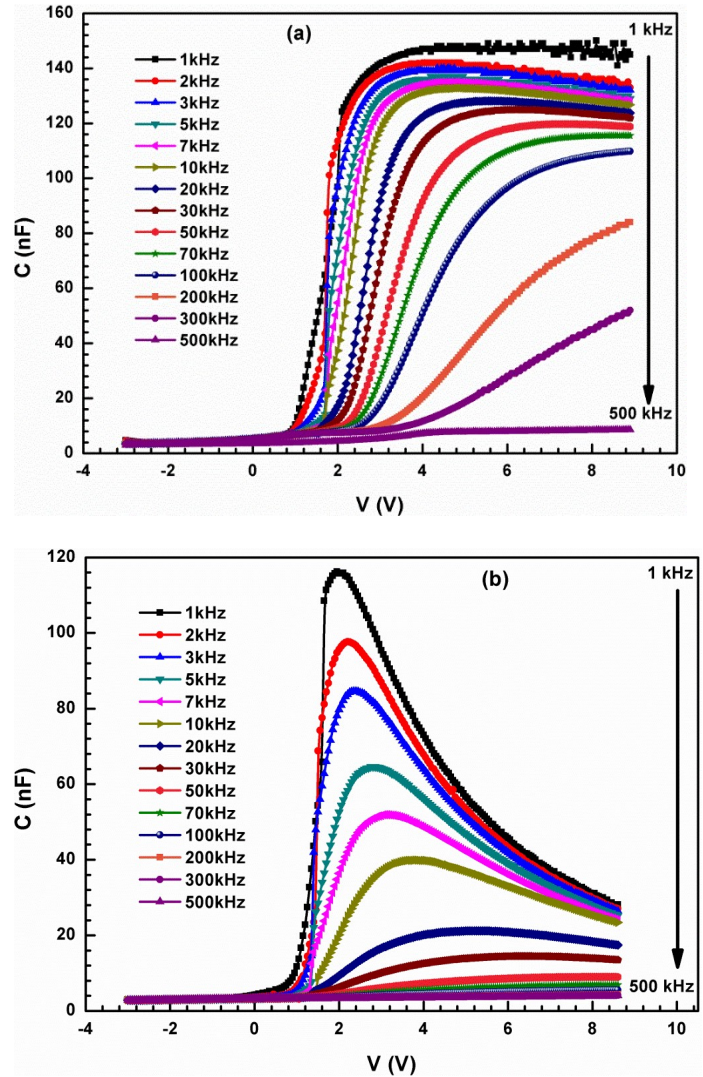


Figure 1 Frequency dependent plot of the $C-V$ characteristics of (a) Au/n-SiC and (b) Au/Al₂O₃/n-SiC structures

As it can be seen in Fig 1 (b); inversion takes place in the voltage range of (-3 V) - (1 V), depletion is in (1 V) - (5 V), and finally accumulation region is in the range of (5 V) - (9 V) capacitance-voltage curves. These regions can be clearly seen in Fig. 1 (b). However, inversion and depletion regions are dominant in Fig. 1 (a). Fig. 1 (b) shows that capacitance behavior at particularly low frequencies (1 kHz-10 kHz) gives a strong peak in the depletion region for MIS structure. This peak can be attributed to the interfacial distribution of metal-insulator-semiconductor interfaces, the series resistance, and the density of the interface insulation layer [32]. For both structures, the increase in $C-V$ values, in the depletion region can be attributed to the presence of interfacial states at low frequencies. Moreover, the separation of $C-V$ curves in the accumulation region,

can also be attributed to the value and magnitude of series resistance at high frequencies [33].

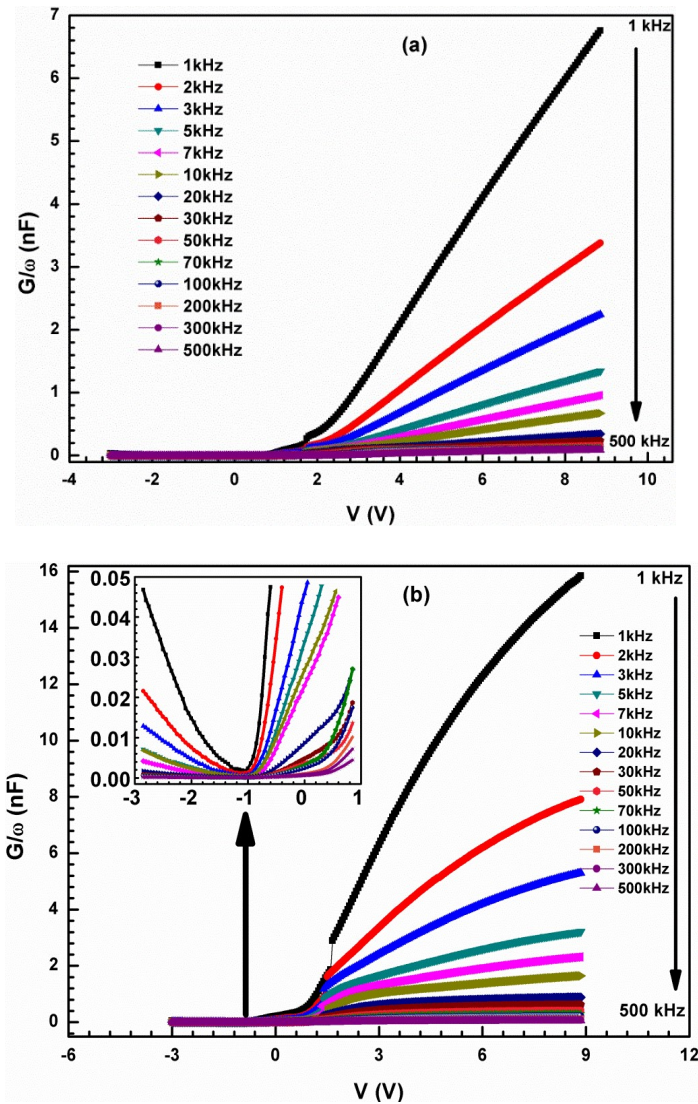


Figure 2 Frequency dependent plot of the G/ω - V characteristics of (a) Au/n-SiC and (b) Au/Al₂O₃/n-SiC structures

Figs. 2 (a) and (b) illustrate that the variation in conductivity (G/ω - V) the forward (9 V) and the reverse (-3V) bias voltage for the same frequency ranges show similar behaviors to the C - V variations in Figs. 1 (a) and (b). The separation occurring in the C - V and G/ω - V characteristics, can be ascribed to the presence of interface state densities (N_{ss}) and their different carrier lifetimes (τ) at low frequencies in the depletion region. While the interface charges can follow the AC signal at low frequencies, these charges cannot follow the AC signal on high frequencies (the carrier life time τ is much larger than $1/2\pi f$ are reached) [11, 33]. Both

C and G/ω values decrease with increasing frequency, the changing C and G/ω values are considerably higher at low frequencies than at higher frequencies. The inset in Fig. 2 (b) exhibits G/ω - V characteristics of Au/Al₂O₃/n-SiC structure in inversion region. As can be seen from this inset, G/ω - V characteristics of Au/Al₂O₃/n-SiC structure in inversion region shows U-shaped behavior. This proves that Au/Al₂O₃/n-SiC structures do not have conductive properties at -1 V due to the fact that all free charges are caught in traps.

The carrier lifetime is much larger than the inverse of the angular frequencies and the charges in the interface cannot follow the AC signal. In such cases, the capacitance and conductance decrease as the frequency increases [34].

The electrical performance of devices such as MS, and MIS depends on crucially the properties of dielectric parameters. Therefore, all properties belong to the dielectric parameters such as electrical modulus, real and imaginary parts of (ϵ' , ϵ'') of complex permittivity (ϵ^*), and $\tan\delta$ for Au/n-SiC (MS) and Au/Al₂O₃/n-SiC MIS structures have been examined with all details by using C and G/ω results in the frequency steps from 1 kHz to 500 kHz and applying voltage sweep from forward (9V) to reverse (-3V) at 300 K.

The dielectric spectroscopy method has been commonly used to determine the dielectric properties of MS and MIS structures in the literature [35, 36]. The ϵ^* is the most basic point in this method and it is defined with the formula below [33, 34]:

$$\epsilon^* = \epsilon' - i\epsilon'' \quad (1)$$

The real part ϵ' and imaginary part ϵ'' parameters were acquired from voltage and frequency dependent C and G/ω analyses by using the formulas below [36]:

$$\epsilon' = \frac{C}{C_0} \quad (2)$$

$$\epsilon'' = \frac{G/\omega}{C_0} \quad (3)$$

In Eqs. 2 and 3, $C_0 (= \epsilon_0 A/d_i)$ is the empty capacitor, ϵ_0 is the permittivity of free-space or vacuum, d_i is the thickness of insulator layer and A is the rectifier contact area of device.

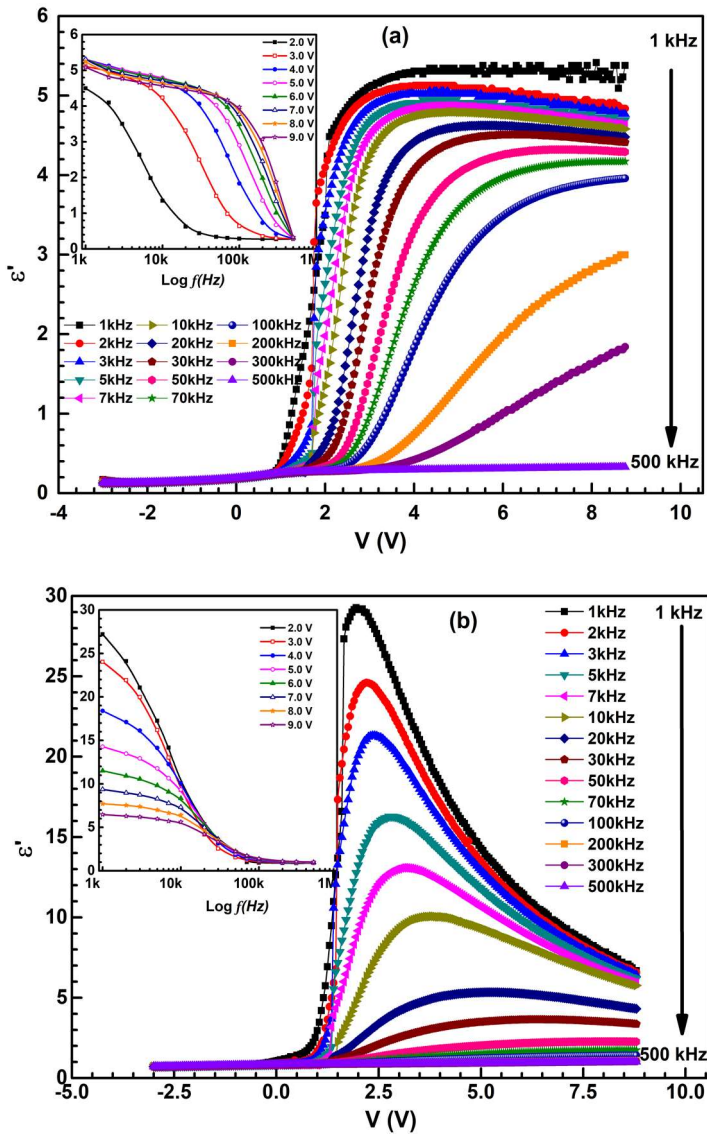


Figure 3 The frequency and voltage dependent comparative plots of the dielectric constant (ϵ') in the depletion region of (a) Au/n-SiC and (b) Au/Al₂O₃/n-SiC structures

Fig. 3 exhibits the ϵ' -V and ϵ' -logf (inset figure) graphs for MS and MIS structures. According to inset figure of Fig. 3, ϵ' sharply decreases between 1 kHz and 100 kHz at low voltages, while ϵ' decreases between 100 kHz and 500 kHz at high voltages for Au/n-SiC structures. Moreover, ϵ' sharply decreases between 1 kHz and 100 kHz at all voltages, while its value is almost the same constant value from 100 kHz to 500 kHz for Au/Al₂O₃/n-SiC

structures. There is an exponential decrease for both the Au/n-SiC and the Au/Al₂O₃/n-SiC structures. Fig. 3 also exhibits that the value of the ϵ' is as low as about four times by means of the interfacial insulating layer at the low frequency region. The graph of ϵ' -logf shows that ϵ' values decrease with increasing frequency. As can be understood from the inset graph of Fig. 3 (a), ϵ' values in MS structure increase with increasing voltage, while the ϵ' values in MIS decrease with increasing voltage in the inset graph of Fig. 3 (b).

Comparing the Fig. 3 (a) and (b), it should also be noted that the MIS structure provides a dielectric increase due to the insulating interface. Dielectric interfaces are expected to increase dielectric constant. In the MS and MIS structures, ϵ' commonly decreases as frequency increases. This decrease in ϵ' due to the increase in frequency stems from the factors such as the orientation of molecules, interface polarization and ionic polarization [34]. The value of the dielectric constant decreases as the alignment of the dipoles at higher frequencies is faster [37].

Fig. 4 exhibits the ϵ'' -V and ϵ'' -logf (inset figure) graphs for MS and MIS structures. According to inset figure of Fig. 4, ϵ'' sharply decreases between 1 kHz and 10 kHz at all voltages for Au/n-SiC and Au/Al₂O₃/n-SiC structures. The ϵ'' is almost the same constant value from 100 kHz to 500 kHz in the accumulation region for Au/n-SiC and Au/Al₂O₃/n-SiC structures. There is an exponential decrease for both the Au/n-SiC and the Au/Al₂O₃/n-SiC structures. Just as the Fig. 3, the Fig. 4 shows that there is a decrease in the imaginary dielectric constant with frequency, while it exhibits an increase with voltage especially in the depletion region. The characteristic behavior in Fig. 4 demonstrates that the energy distribution of the MS and MIS constructions decrease as the frequency increases [38].

Fig. 4 also demonstrates that the value of the ϵ'' is as low as about four times by means of the interfacial insulating layer at the low frequency region. The dipoles in the insulator material can be polarized under an external applied bias voltage or an electric field that displaces the charges from their equilibrium position or traps at low and medium

frequencies. This explains the evolution of dielectric performance as a consequence of relaxation time [37, 38]. On the other hand, the change of dielectric loss starts in the depletion and accumulation regions. Namely there is no change in dielectric loss due to no energy loss in inversion region. ϵ' and ϵ'' values are compatible with the results obtained in similar studies in the literature [38].

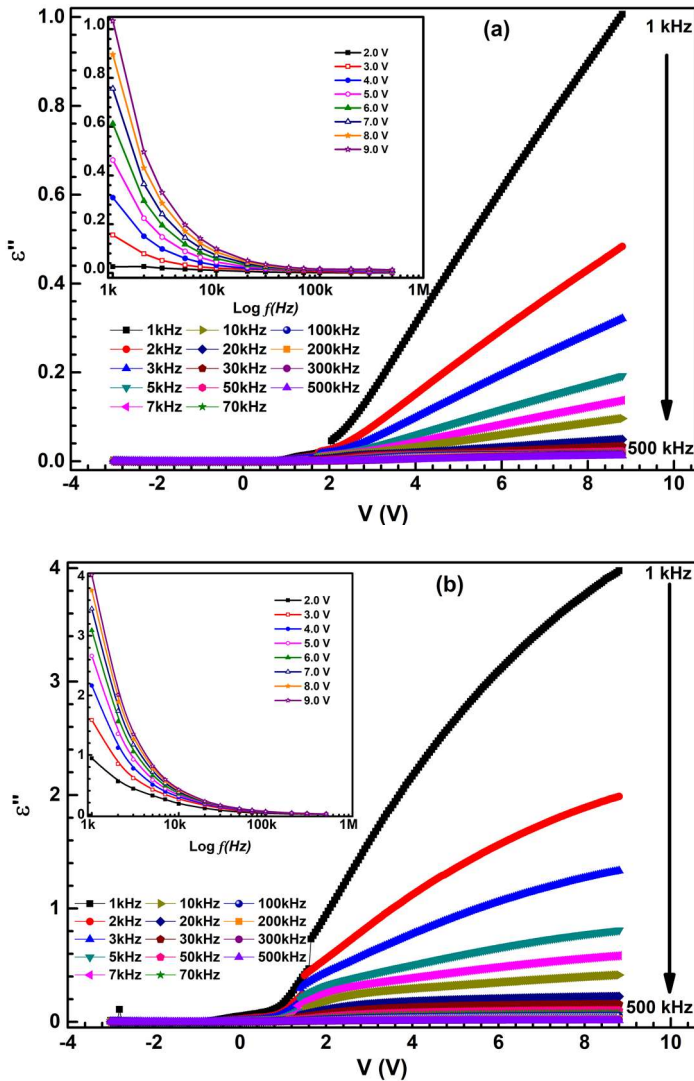


Figure 4 The frequency and voltage dependent comparative plots of the dielectric loss (ϵ'') in the depletion region of (a) Au/n-SiC and (b) Au/Al₂O₃/n-SiC structures

The experimental results in this research demonstrate that both dipole and interface polarizations can easily occur at low frequencies and trapped charges can follow the AC signal. In such a case, the dielectric loss in the inversion region does not change even if the frequency

increases. Therefore, the dielectric loss in the inversion remains almost constant.

The $\tan\delta$ is expressed in the formula below [36]:

$$\tan\delta = \frac{\epsilon''}{\epsilon'} \quad (4)$$

Fig. 5 exhibits the $\tan\delta$ -V and $\tan\delta$ -logf (inset figure) graphs for MS and MIS structures. According to inset figure of Fig. 5, $\tan\delta$ rapidly decreases between 1 kHz and 10 kHz at all voltages for Au/n-SiC and Au/Al₂O₃/n-SiC structures.

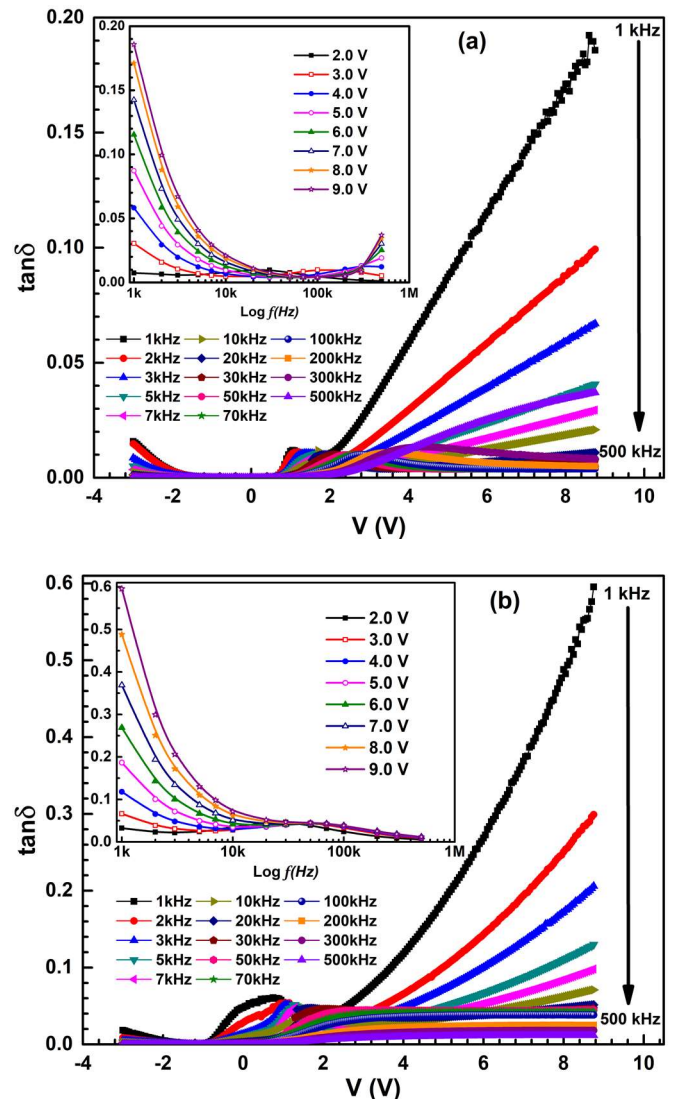


Figure 5 The frequency and voltage dependent comparative plots of the loss tangent ($\tan\delta$) in the depletion region of (a) Au/n-SiC and (b) Au/Al₂O₃/n-SiC structures

The $\tan\delta$ has almost the same constant value from 10 kHz to 500 kHz for Au/n-SiC and Au/Al₂O₃/n-

SiC structures. There is an exponential decrease for both the Au/n-SiC and the Au/Al₂O₃/n-SiC structures. The $\tan\delta$ -V (Fig. 5) and $\tan\delta$ -logf diagrams (Fig. 5 inset), which are determined based on both ε' and ε'' values, exhibit peak behavior in the medium frequency domain (10 kHz-100 kHz) and in the depletion region for the MIS structure, while MS structure exhibits peak behavior in the high frequency domain and in the depletion region (between 1 V and 5V) [39].

While frequency increases, $\tan\delta$ -logf (inset figure) values decrease. The peak position for the MS and MIS structures has shifted towards the middle frequency region due to the restructuring and rearrangement of the surface state. The Fig. 5 also shows that there is a decrease in the loss tangent with frequency, while it exhibits an increase with voltage, especially in the depletion region. This increase begins after 5 V for MS structure, while it begins after 3 V. On the other hand, it is well known that the interfacial properties of C and G/ω are extremely sensitive to the properties and are the effect of R_s [39]. It is seen that surface state density and interface polarization values affect the $\tan\delta$ -V and the $\tan\delta$ -logf characteristic values when a bias voltage is applied to MS and MIS structure according to the literature [40]. This peak behavior in the $\tan\delta$ -V and the $\tan\delta$ -logf plots can only be attributed to the interface states. Bulk phenomenon in complex systems can easily be interpreted by means of electrical modulus formalism. The evaluation of the electrical modulus as a function of the frequency gives rise to understand the relaxation processes in the studied materials. The Complex dielectric data are converted to the M^* equation using the following formula [41]:

$$M^* = \frac{1}{\varepsilon^*} = M' + jM'' = \frac{\varepsilon'}{\varepsilon'^2 + \varepsilon''^2} + \frac{\varepsilon''}{\varepsilon'^2 + \varepsilon''^2} \quad (5)$$

Here, j is the imaginary root (-1), M' and M'' are respectively the real and the imaginary parts of complex modulus. Fig. 6 (a) and (b) indicate the M' -V graph while Fig. 6 (c) and (d) indicate M'' -V plots for MS and MIS structures. The value of M' for MS structure changes between 6.0 and 8.0 in inversion region, while it changes between 0.3 and 4.5 as rising from low frequency to high frequency in depletion and accumulation regions. The value of

M' for MIS structure changes between 1.2 and 1.4 in inversion region, while it changes between 0.1 and 1.2 as rising from low frequency to high frequency in depletion and accumulation regions. When Fig. 6 (a) and (b) are examined, the rise of M' values of MS and MIS structures with increasing frequency in depletion region is observed. The values of M' in the reverse bias exhibit independent behavior from frequency. So the characteristics of the real electrical modulus versus frequency only in the depletion region have been investigated. It is also indicated that there is an increase with the frequency and a decrease with the voltage in the internal graphics of Fig. 6 (a) and (b). The polarization effect may cause these characteristic behaviors to occur in MS and MIS.

In addition, the electrical modulus values reach their maximum level at high frequencies due to the relaxation processes [42]. This can be explained as the almost zero approximation of M' values at low frequencies. In the Fig. 6 (a) and (b), especially about 100 kHz for MS structure and 10 kHz for MIS structure, M' increases rapidly as frequency increases. From 100 kHz to 500 kHz for MS structure and from 10 kHz to 500 kHz for MIS structure, the conduction mechanism can be positively affected by the short-range mobility of the charge carriers in the interfaces of structures. This indicates that there is no restoring force under the influence of a constant electric field. That means, the charge flow may not occur. [43]. The value of M'' for MS structure changes between 0.01 and 0.095 in inversion region, while it changes between 0 and 0.035 in depletion region and between 0 and 0.040 accumulation regions. The value of M'' for MIS structure changes between 0 and 0.035 in inversion region, while it changes between 0 and 0.05 in depletion region and between 0.01 and 0.065 accumulation regions. In the Fig. 6 (c) and (d), the M'' -V plot has a peak point for both samples in a given voltage range. The voltage ranges from bottom to the peak positions of the M'' -V characteristics with increasing frequency to determine the distance that the load carriers are mobile at long distances.

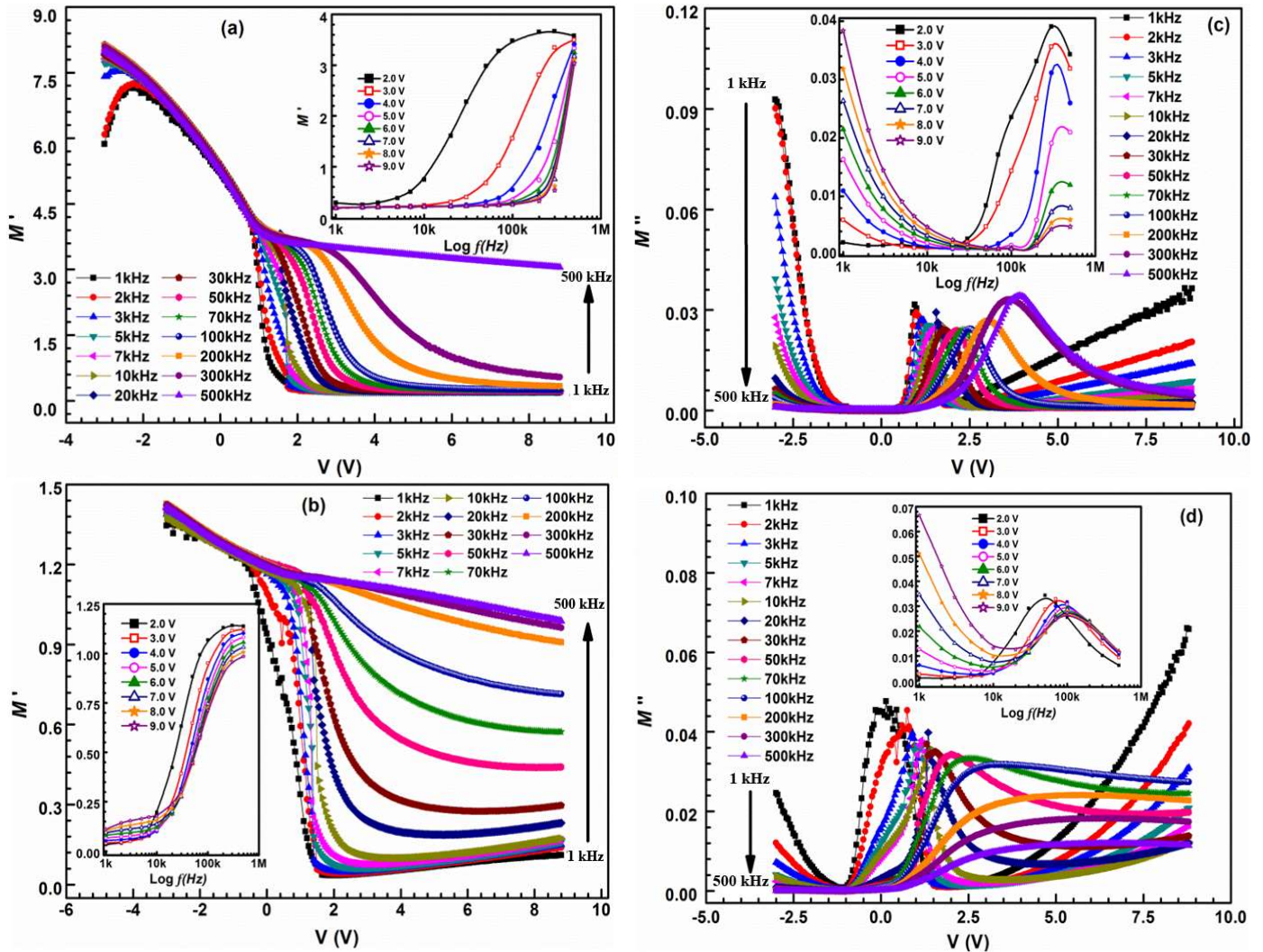


Figure 6 (a) and (b) characteristics of the real electrical modulus for Au/n-SiC and Au/Al₂O₃/n-SiC structures, respectively. (c) and (d) characteristics of the imaginary electrical modulus for Au/n-SiC and Au/Al₂O₃/n-SiC structures, respectively

The values in both the reverse and forward bias exhibit frequency dependent behavior. There is also a decrease with increasing frequency in the reverse bias region.

However, peak distribution in the imaginary electrical modulus of both samples exhibit only in the depletion region. So the characteristics of the imaginary electrical modulus versus frequency only in the depletion region have been investigated. In this study the Fig. 6 (c) and (d) shows that there is a decrease with the frequency. Moreover, there is an increase with the voltage at low frequency region, while there is a decrease with voltage at high frequency region in the internal graphics.

On the other hand, a very distinct peak is seen in the internal graph of Fig.6 (d) and increasing voltage

shifts the peak position towards the high frequency region. This characteristic change in the imaginary electrical modulus of the insulator interfacial material can be attributed to surface polarization effects and the relaxation mechanism of dipoles formed between semiconductor and insulator [41]. Otherwise, the peak position of M'' shifts to the left due to the effect of the insulating layer since, the insulating layer reduces the contribution to the values of ϵ' and ϵ'' by regulating the interface states. By means of the insulation layer, the shifting modulus peak also contributes significantly to the correlation between the mobility of the moving load carriers [43]. M' and M'' values are compatible with the results obtained in similar studies in the literature [24, 38].

The frequency and voltage dependent AC electrical conductivity of both MS and MIS structures are given by the following formula [33] and the characteristic in the depletion region is exhibited in Fig. 7.

$$\sigma_{ac} = \omega C \tan \delta (d/A) = \varepsilon'' \omega \varepsilon_0 \quad (6)$$

It is also seen in the Fig. 7 (b), σ_{ac} reaches to higher values by means of interfacial layer. Compared the Fig. 7 (a) and (b), it is also clear that the MIS structure has higher conductivities than MS. The increase in AC conductivity can be ascribed to the characterization of the loss tangent as well as to the reduction of defects at interfaces with increasing frequency [44].

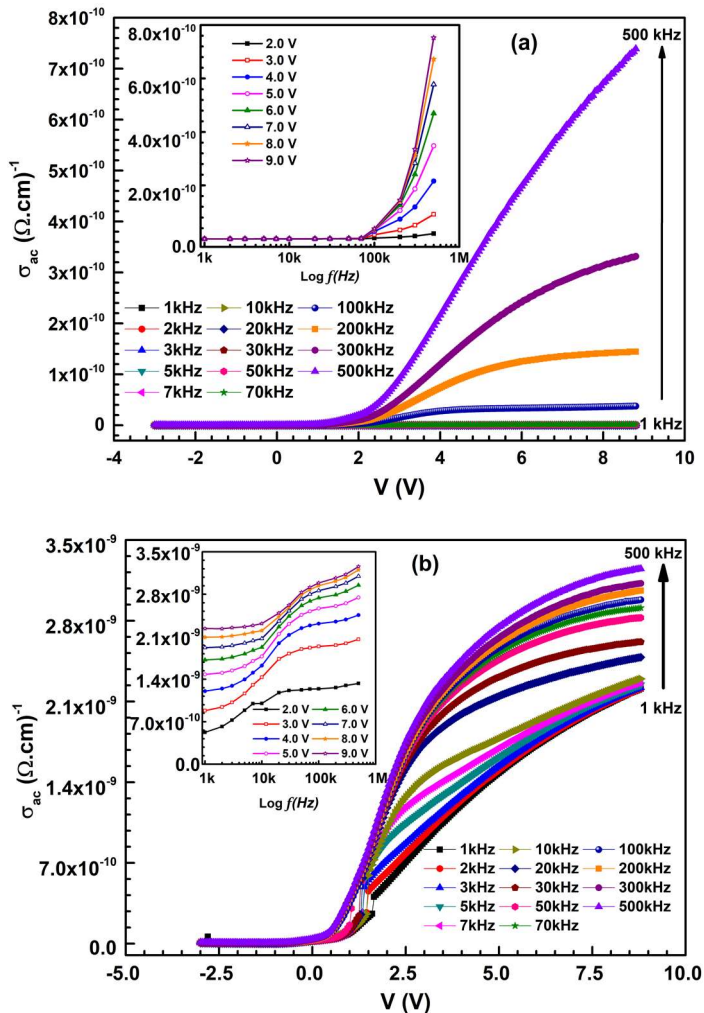


Figure 7 The frequency and voltage dependent comparative plots of the ac electrical conductivity (σ_{ac}) in the depletion region of (a) Au/n-SiC and (b) Au/Al₂O₃/n-SiC structures

It is obviously seen from Fig. 7 (a) and (b) that AC electrical conductivity has higher values in the

depletion and accumulation regions. Then, it is saturated in the accumulation region (high forward bias) due to series resistance of samples. Moreover, σ_{ac} increases as the frequency increases. This characteristic change in the σ_{ac} can be ascribed to the increase of surface polarization effects with increasing frequency and the occurrence of series resistance in the high voltage region [45]. As a result, these characteristic behaviors that the dielectric properties were developed by means of the Al₂O₃ layer effect.

4. CONCLUSION

In this study, Au/n-SiC Metal-semiconductor (MS) and Au/Al₂O₃/n-SiC Metal-Insulator-Semiconductor (MIS) structures were produced to investigate the electric and dielectric properties at room temperature. For this research, the dielectric characteristics of the structures were carried out by applying a (-3V) - (9V) bias voltage at a frequency range of 1 kHz-500 kHz and at room temperature. Al₂O₃ (70 Å thick) was used as a high dielectric interfacial insulating layer between the metal and the semiconductor to enhance the performance of the MIS structure compared with the MS structure. It is evident that the dielectric parameters strongly depend on the frequency and voltage in the depletion and accumulation regions mainly due to the interface polarization and interface traps. The obtained results show that each of the parameters ε' , ε'' and $\tan \delta$ exhibits a sharp decrease with increasing frequency due to the applied bias voltage, whereas real part of electrical modulus characteristics increase with increasing frequency at high forward bias region. However, imaginary part of electrical modulus characteristics decreases with increasing frequency at low reverse bias region. The high frequency variation in ε' and ε'' can be ascribed to Maxwell-Wagner and field charge polarization. The larger values of ε' may depend on the dielectric properties of the insulator Al₂O₃ and the trapped electron density at the interfaces between MS and MIS structures. The M'' has a peak point for both structures in a given frequency range. The frequency ranges from the bottom to peak position of the M'' characteristics determine the mobile distances of the charge carriers at long distances. Otherwise, the peak position of M'' shifts to the left due to the effect of the insulating layer.

We believe this study will clarify the characteristics of MIS capacitors and help in finding solutions to some problems in interface states due to the fact that minimizing the interface states between metal-semiconductor on MIS structure with high dielectric material Al_2O_3 . Hence, our method in this study will considerably contribute to the production of electronic devices with metal-insulator-semiconductor. In addition, it is thought that such materials will increase the current level of MIS electronic devices in the future due to the minimum interface conditions. In conclusion, the Al_2O_3 interface insulating layer leads to a significant improvement in capacitance and dielectric constant compared to SiO_2 so that more charge or energy can be stored.

Funding

This work was supported by the Düzce University Scientific Research Projects [Project number: 2013.07.02.204]

The Declaration of Conflict of Interest / Common Interest

No conflict of interest or common interest has been declared by the authors.

Authors' Contribution

In this study, the contributions of the authors in the research, writing and Review & Editing stages are equal.

The Declaration of Ethics Committee Approval

The authors declare that this document does not require an ethics committee approval or any special permission.

The Declaration of Research and Publication Ethics

The authors of the paper declare that they comply with the scientific, ethical and quotation rules of SAUJS in all processes of the paper and that they do not make any falsification on the data collected. In addition, they declare that Sakarya University Journal of Science and its editorial board have no

responsibility for any ethical violations that may be encountered, and that this study has not been evaluated in any academic publication environment other than Sakarya University Journal of Science.

REFERENCES

- [1] J. Zhang, G. Zhao, Y. Li, Y. Li, and W. Liu, "Effect of Al-Zr co-doping on the electrical properties of graphene/ZnO Schottky contact," *Materials Research Express*, vol. 6, no. 12, pp. 125911, 2020.
- [2] A. Demir, İ. Yücedağ, G. Ersöz, Ş. Altındal, N. Baraz, and M. Kandaz, "A Comparative Study on the Main Electrical Parameters of Au/n-Si, Au/Biphenyl-CuPc/n-Si and Au/Biphenylsub-CoPc/n-Si Type Schottky Barrier Diodes," *Journal of Nanoelectronics and Optoelectronics*, vol. 11, no. 5, pp. 620-625, 2016.
- [3] Ç. S. Güçlü, A. F. Özdemir, A. Kökce, and Ş. Altındal, "Frequency and Voltage-Dependent Dielectric Properties and AC Electrical Conductivity of (Au/Ti)/ Al_2O_3 /n-GaAs with Thin Al_2O_3 Interfacial Layer at Room Temperature," *Acta Physica Polonica A*, vol. 130, no. 1, pp. 325-330, 2016.
- [4] N. Kumar and S. Chand, "Effects of temperature, bias and frequency on the dielectric properties and electrical conductivity of Ni/ SiO_2 /p-Si/Al MIS Schottky diodes," *Journal of Alloys and Compounds*, vol. 817, pp. 153294, 2020.
- [5] S. M. Sze and K. K. Ng "Physics of semiconductor devices," New York: John Wiley & Sons, 2006.
- [6] E. H. Rhoderick and R. H. Williams, "Metal Semiconductor Contacts," Oxford: Oxford University Press, 1988.

- [7] E. H. Nicollian and J. R. Brews, "MOS (metal oxide semiconductor) physics and technology," New York: John Wiley & Sons, 1982.
- [8] Y. Zhou, M. Ogawa, X. Han, and K. Wang, "Alleviation of Fermi-level pinning effect on metal/germanium interface by insertion of an ultrathin aluminum oxide," *Applied Physics Letters*, vol. 93, no. 20, pp. 202105(1-3), 2008.
- [9] S. Zheng, W. Yang, Q. Sun, L. Chen, P. Zhou, P. Wang, D. Zhang, and F. Xiao, "Schottky barrier height reduction for metal/n-InP by inserting ultra-thin atomic layer deposited high-k dielectrics," *Applied Physics Letters*, vol. 103, no. 26, pp. 261602(1-4), 2013.
- [10] Ç. G. Türk, S. O. Tan, Ş. Altındal, and B. İnem, "Frequency and voltage dependence of barrier height, surface states, and series resistance in Al/Al₂O₃/p-Si structures in wide range frequency and voltage," *Physica B: Condensed Matter*, vol. 582, pp. 411979(1-8), 2020.
- [11] A. Baradeswaran and A. E. Perumal, "Study on mechanical and wear properties of Al 7075/Al₂O₃/graphite hybrid composites," *Composites Part B: Engineering*, vol. 56, pp. 464-471, 2014.
- [12] M. W. Akhtar, Y. S. Lee, D. J. Yoo, and J. S. Kim, "Alumina-graphene hybrid filled epoxy composite: Quantitative validation and enhanced thermal conductivity," *Composites Part B: Engineering*, vol. 131, pp. 184-195, 2017.
- [13] S. Hlali, N. Hizem, and A. Kalboussi, "High-k dielectric materials for the gate oxide of a MIS capacitor: effect of interface states on the C-V characteristics," *Journal of Computational Electronics*, vol. 15, no. 4, pp. 1340-1350, 2016.
- [14] G. D. Wilk, R. M. Wallace, and J. M. Anthony, "High-κ gate dielectrics: Current status and materials properties considerations," *Journal of Applied Physics*, vol. 89, no. 10, pp. 5243-5275, 2001.
- [15] D. Shahrjerdi, E. Tutuc, and S. K. Banerjee, "Impact of surface chemical treatment on capacitance-voltage characteristics of GaAs metal-oxide-semiconductor capacitors with Al₂O₃ gate dielectric," *Applied Physics Letters*, vol. 91, no. 6, pp. 063501(1-4), 2007.
- [16] D. Hoogeland, K. B. Jinesh, F. Roozeboom, W. F. Besling, M. C. M. Van De Sanden, and W. M. M. Kessels, "Plasma-assisted atomic layer deposition of TiN/Al₂O₃ stacks for metal-oxide-semiconductor capacitor applications," *Journal of Applied Physics*, vol. 106, no. 11, pp. 114107(1-7), 2009.
- [17] Y. Xuan, P. D. Ye, and H. C. Lin, "Minority-carrier characteristics of InGaAs metal-oxide-semiconductor structures using atomic-layer-deposited Al₂O₃ gate dielectric," *Applied Physics Letters*, vol. 89, no. 13, pp. 132103(1-3), 2006.
- [18] G. Dingemans and W. M. M. Kessels, "Aluminum oxide and other ALD materials for Si surface passivation," *ECS Transactions*, vol. 41, no. 2, pp. 293-301, 2011.
- [19] J. Benick, A. Richter, M. Hermle, and S. W. Glunz, "Thermal stability of the Al₂O₃ passivation on p-type silicon surfaces for solar cell applications," *Physica Status Solidi-Rapid Research Letters*, vol. 3, no. 7-8, pp. 233-235, 2009.
- [20] G. Agostinelli, A. Delabie, P. Vitanov, Z. Alexieva, H. F. W. Dekkers, S. De Wolf, and G. Beaucarne, "Very low surface recombination velocities on p-type silicon wafers passivated with a dielectric with fixed negative charge,"

- Solar Energy Materials & Solar Cells, vol. 90, no. 18-19, pp. 3438-3443, 2006.
- [21] J. Schmidt, A. Merkle, R. Brendel, B. Hoex, M. C. M. Van De Sanden, and W. M. M. Kessels, "Surface passivation of high-efficiency silicon solar cells by atomic-layer-deposited Al_2O_3 ," *Progress in Photovoltaics: Research and Applications*, vol. 16, no. 6, pp. 461-466, 2008.
- [22] J. A. Cooper and A. Agarwal, "SiC power-switching devices-the second electronics revolution?," *Proceedings of the Institution of Electrical Engineers*, vol. 90, no. 6, pp. 956-968, 2002.
- [23] R. J. Trew, J. Yan, and P. M. Mock, "The potential of diamond and SiC electronic devices for microwave and millimeter-wave power applications," *Proceedings of the Institution of Electrical Engineers*, vol. 79, no. 5, pp. 598-620, 1991.
- [24] S. Hlali, A. Farji, N. Hizem, L. Militaru, A. Kalboussi, and A. Souifi, "High temperature and voltage dependent electrical and dielectric properties of $\text{TiN}/\text{Al}_2\text{O}_3/\text{p-Si}$ MIS structure," *Journal of Alloys and Compounds*, vol. 713, pp. 194-203, 2017.
- [25] S. Parui, A. Atxabal, M. Ribeiro, A. Bedoya-Pinto, X. Sun, R. Llopis, F. Casanova, and L. E. Hueso, "Reliable determination of the Cu/n-Si Schottky barrier height by using in-device hot-electron spectroscopy," *Applied Physics Letters*, vol. 107, no. 18, pp. 183502(1-5), 2015.
- [26] H. Kim, Y. Kim, and B. J. Choi, "Interfacial characteristics of $\text{Au}/\text{Al}_2\text{O}_3/\text{InP}$ metal-insulator-semiconductor diodes," *American Institute of Physics Advances*, vol. 8, no. 9, pp. 095022(1-8), 2018.
- [27] Ç. Ş. Güçlü, A. F. Özdemir, A. Karabulut, A. Kökçe, and Ş. Altındal, "Investigation of temperature dependent negative capacitance in the forward bias C-V characteristics of $(\text{Au}/\text{Ti})/\text{Al}_2\text{O}_3/\text{n-GaAs}$ Schottky barrier diodes (SBDs)," *Materials Science in Semiconductor Processing*, vol. 89, pp. 26-31, 2019.
- [28] F. Zhang, G. Sun, L. Zheng, S. Liu, B. Liu, L. Dong, L. Wang, W. Zhao, X. Liu, G. Yan, L. Tian, and Y. Zeng, "Interfacial study and energy-band alignment of annealed Al_2O_3 films prepared by atomic layer deposition on 4H-SiC," *Journal of Applied Physics*, vol. 113, no. 4, pp. 044112, 2013.
- [29] E. Schilirò, R. L. Nigro, P. Fiorenza, and F. Roccaforte, "Negative charge trapping effects in Al_2O_3 films grown by atomic layer deposition onto thermally oxidized 4H-SiC," *AIP Advances*, vol. 6, no. 7, pp. 075021, 2016.
- [30] C. M. Tanner, Y.-C. Perng, C. Frewin, S. E. Saddow, and J. P. Chang, "Electrical performance of Al_2O_3 gate dielectric films deposited by atomic layer deposition on 4 H-Si C," *Applied Physics Letters*, vol. 91, no. 20, pp. 203510, 2007.
- [31] G. Ersöz, İ. Yücedağ, Y. Azizian-Kalandaragh, I. Orak, and Ş. Altındal, "Investigation of electrical characteristics in $\text{Al}/\text{CdS-PVA}/\text{p-Si}$ (MPS) structures using impedance spectroscopy method," *Ieee Transactions on Electron Devices*, vol. 63, no. 7, pp. 2948-2955, 2016.
- [32] İ. Yücedağ, "On the anomalous peak at low and moderate frequency C-V curves of $\text{Al}/\text{SiO}_2/\text{p-Si}$ structure at the forward bias region," *Optoelectronics and Advanced Materials-Rapid Communications*, vol. 3, no. 6, pp. 612-615, 2009.
- [33] A. Gümüş, G. Ersöz, İ. Yücedağ, S. Bayrakdar, and Ş. Altındal, "Comparative study of the temperature-dependent dielectric properties of

- Au/PPy/n-Si (MPS)-type Schottky barrier diodes,” *Journal of the Korean Physical Society*, vol. 67, no. 5, pp. 889-895, 2015.
- [34] N. Baraz, İ. Yücedağ, Y. Azizian-Kalandaragh, G. Ersöz, İ. Orak, Ş. Altındal, B. Akbari, and H. Akbari, “Electric and dielectric properties of Au/ZnS-PVA/n-Si (MPS) structures in the frequency range of 10-200 kHz,” *Journal of Electronic Materials*, vol. 46, no. 7, pp. 4276-4286, 2017.
- [35] F. I. H. Rhouma, A. Dhahri, J. Dhahri, and M. A. Valente, “Dielectric, modulus and impedance analysis of lead-free ceramics $Ba_{0.8}La_{0.133}Ti_{1-x}Sn_xO_3$ ($x=0.15$ and 0.2),” *Applied Physics A Materials Science & Processing*, vol. 108, no. 3, pp. 593-600, 2012.
- [36] N. Shiwakoti, A. Bobby, K. Asokan, and B. Antonya, “Temperature dependent dielectric studies of Ni/n-GaP Schottky diodes by capacitance and conductance measurements,” *Materials Science in Semiconductor Processing*, vol. 42, pp. 378-382, 2016.
- [37] H. N. Chandrakala, B. R. Shivakumaraiah, and G. M. M. Siddaramaiah, “The influence of zinc oxide-cerium oxide nanoparticles on the structural characteristics and electrical properties of polyvinyl alcohol films,” *Journal of Materials Science*, vol. 47, no. 23, pp. 8076-8084, 2012.
- [38] D. E. Yıldız, M. Yıldırım, and M. Gökçen, “Investigation on dielectric properties of atomic layer deposited Al_2O_3 dielectric films,” *Journal of Vacuum Science & Technology A*, vol. 32, no. 3, pp. 031509(1-5), 2014.
- [39] İ. Yücedağ, A. Kaya, and Ş. Altındal, “On the frequency dependent negative dielectric constant behavior in Al/Co-doped (PVC+TCNQ)/p-Si structures,” *International Journal of Modern Physics B*, vol. 28, no. 23, pp. 1450153(1-15), 2014.
- [40] İ. Yücedağ, A. Kaya, H. Tecimer, and Ş. Altındal, “Temperature and voltage dependences of dielectric properties and ac electrical conductivity in Au/PVC+TCNQ/p-Si structures,” *Materials Science in Semiconductor Processing*, vol. 28, pp. 37-42, 2014.
- [41] A. Kaya, İ. Yücedağ, H. Tecimer, and Ş. Altındal, “A comparative electric and dielectric properties of Al/p-Si structures with undoped and Co-doped interfacial PVA layer,” *Materials Science in Semiconductor Processing*, vol. 28, pp. 26-30, 2014.
- [42] Y. Şafak Asar, T. Asar, Ş. Altındal, and S. Özçelik, “Investigation of dielectric relaxation and ac electrical conductivity using impedance spectroscopy method in (AuZn)/TiO₂/p-GaAs(110) schottky barrier diodes,” *Journal of Alloys and Compounds*, vol. 628, no. 442-449, 2015.
- [43] T. Badapanda, S. Sarangi, S. Parida, B. Behera, B. Ojha, and S. Anwar, “Frequency and temperature dependence dielectric study of strontium modified Barium Zirconium Titanate ceramics obtained by mechanochemical synthesis,” *Journal of Materials Science: Materials in Electronics*, vol. 26, no. 5, pp. 3069-3082, 2015.
- [44] M. N. Siddique, A. Ahmed, and P. Tripathi, “Dielectric relaxation and Hopping conduction mechanism in $Ni_{1-x}Sr_xO$ nanostructures,” *Materials Chemistry and Physics*, vol. 239, pp. 121959, 2020.
- [45] S. Kraiem, K. Khirouni, and S. Alaya, “AC electrical properties of Schottky diode based on nanocrystalline silicon thin films,” *Physica B: Condensed Matter*, vol. 584, pp. 412108, 2020.